

Design of a Low-Orbit-to-Geostationary Satellite Link for Maximal Throughput

William E. Ryan, Li Han, and Paul A. Quintana

Abstract— We examine the design of a communication link involving the data transfer from a small, low-orbit satellite to a ground station, but through a geostationary satellite. The advantage of this approach is that a single ground station, which tracks only the geostationary satellite, may be shared by a multiplicity of small satellites. Our goal is to select certain small satellite parameters—signaling rate, small satellite antenna beamwidth, modulation scheme and coding scheme—which maximize the data throughput in bits/day. Our approach uses orbital simulations of this scenario together with theoretical analysis based on the channel capacity C and cutoff rate R_0 . The throughput achievable by several practical coding schemes is also examined.

Index Terms—Capacity, cutoff rate, GEO satellites, LEO satellites, time-varying channels, time-varying codes.

I. INTRODUCTION

THE introduction of small low-earth-orbit (LEO) satellites for the investigation of near-earth phenomena and other applications has prompted the study of data transfer methods from the satellite to its users on the ground. The most natural method of data transfer is to assign to each small satellite a ground terminal which tracks it as it passes overhead. An alternative has been proposed [1] whereby a communication relay through a geostationary (GEO) satellite to a designated ground terminal is established. This approach has the advantage that a number of small satellites may now share a single (expensive) ground station facility. The disadvantage is that there is a link penalty on the order of 26 dB by going through the GEO satellite as opposed to directly to the ground. On the other hand, in many of these applications, the requirement on the throughput rate (in bits/s) and the daily throughput (in bits/day) do not necessitate the extra 26 dB of C/N_0 .

We consider here only LEO satellites with nongimbaled antennas [2] for the following two reasons. First, it represents a worst case situation, and second, the throughput possible when such inexpensive satellites are employed is of interest to NASA and others. Observe that, with nongimbaled antennas, the small satellite must be stabilized (e.g., spin stabilized), and

a communication contact will be made only in the event that its antenna pattern sweeps past the GEO satellite, which we shall assume is tracking the LEO satellite. Observe also that the link between the two satellites will vary as the LEO satellite comes into view of the GEO satellite and then departs to orbit the earth again. Such a time-varying link gives rise to carrier-power-to-noise density ratio “profiles” $C(t)/N_0$, by which we mean carrier-power-to-noise density ratios which vary as a function of time.

It is our goal in this work to design a small satellite communication system which maximizes the throughput to the ground in bits/day. This performance criterion results from the need to protect against overflow of the LEO satellite’s on-board recorder—the recorder will overflow if the incoming data rate exceeds the outgoing rate (throughput to the ground). Moreover, we are interested in the throughput *per day* as opposed to, say, per contact since, generally, the C/N_0 profile is roughly periodic with a period of one day. The connection between the per-day and the per-contact throughputs is elaborated upon below.

Toward the goal of throughput maximization, we simulate the LEO-to-GEO communication link to arrive at C/N_0 profiles on which we base our small satellite system design. We note that the throughput \mathcal{T} (bits/day) is dependent on the small satellite’s antenna beamwidth B , modulation scheme, signaling rate R_s (which we assume to be constant), and error-control coding scheme \mathbb{C} (which might have a time-varying code rate). The problem then is to choose these parameters such that \mathcal{T} is maximized. We shall focus on M -ary PSK modulation so we need only determine the optimal M .

To find the optimal B , R_s , and M , we involve the use of the channel capacity C and cutoff rate R_0 from information theory [3] as discussed in Section II. The information-theoretic approach described in that section is to be applied to specific C/N_0 profiles which are derived using the orbital simulation program described in Section III. In Section IV, we find the optimal B , R_s , and M corresponding to a specific LEO-to-GEO configuration of interest to NASA. As for the optimal code scheme, we can expect that any code scheme \mathbb{C} that might be considered to be optimal will have unmanageable complexity. Thus, in Section V, we examine the throughput of selected coding schemes, where the throughput increases with increasing code complexity.

II. PARAMETER OPTIMIZATION

That there exist optimal B , R_s , and M which maximize daily throughput \mathcal{T} can be heuristically argued as follows. First, the 3 dB beamwidth B affects the number of contacts

Paper approved by D. P. Taylor, the Editor for Signal Design, Modulation and Detection of the IEEE Communications Society. Manuscript received April 10, 1995; revised January 15, 1997. This work was supported by NASA Grant NAG 5-1491. This paper was presented in part at the 1995 International Conference on Communications, Seattle, WA, June 1995.

W. E. Ryan is with the Klipsh Department of Electrical and Computer Engineering, New Mexico State University, Las Cruces, NM 88003 USA.

L. Han was with the Klipsh Department of Electrical and Computer Engineering, New Mexico State University, Las Cruces, NM 88003 USA. He is now with Samsung Semiconductor, San Jose, CA 95134 USA.

P. A. Quintana was with the Klipsh Department of Electrical and Computer Engineering, New Mexico State University, Las Cruces, NM 88003 USA. He is now with Lockheed-Martin WDL, San Jose, CA 95134 USA.

Publisher Item Identifier S 0090-6778(97)05734-6.

made per day, as well as the duration and strength of the contacts. If the beamwidth is too narrow, only a single, very short contact might be achieved, albeit with a relatively strong signal during the contact. On the other hand, a very broad beamwidth might achieve a contact on almost every orbit, but with a very weak signal in each case. Thus, we would expect that there is some optimal B that is a compromise between these two extremes.

We argue that there exists an optimal channel symbol rate R_s (equivalently, code bit rate $R_c = R_s \log_2 M$) as follows. In practice, carrier recovery for an MPSK signal is difficult for values of $E_c(t)/N_0 = (1/R_c)(C(t)/N_0)$ below about 0 dB [4], so we restrict communication to the region $E_c(t)/N_0 \geq 0$ dB. Now note that, as R_c is increased from some small value, we can expect T to initially increase, but eventually the duration of time that $E_c(t)/N_0$ exceeds 0 dB will approach zero, so that T will tend to zero as well. Hence, there is an optimum value for R_c .

Because we assume no bandwidth limitation in our communication system, the channel in effect becomes a power-limited one. Given this, we can anticipate that the optimal values of M are 2 and 4 since BPSK and QPSK are more energy efficient than 8-ary PSK, etc. Nevertheless, we shall consider 8-ary PSK in our analysis below, and see how the optimality of BPSK and QPSK surfaces in the analysis.

We have now established that $T = T(M, R_c, B)$, and we propose to find the parameters M^* , R_c^* , and B^* which maximize T in the following manner. A given C/N_0 profile (which is a function of B) gives rise to an E_c/N_0 profile through the chosen code bit rate R_c : $E_c(t)/N_0 = (1/R_c)(C(t)/N_0)$. In turn, an E_c/N_0 profile together with the signal set size M gives rise to capacity and cutoff rate profiles $C(t) = C(M, E_c(t)/N_0)$ and $R_0(t) = R_0(M, E_c(t)/N_0)$, respectively.¹ Assuming that $C(t)$ and $R_0(t)$ are both in units of bits/s, we may now define the theoretical throughputs

$$\mathcal{T}_C = \int_{\text{one day}} C(t) dt \quad (\text{bits}) \quad (1)$$

$$\mathcal{T}_{R_0} = \int_{\text{one day}} R_0(t) dt \quad (\text{bits}) \quad (2)$$

and observe that both are functions of M, R_c , and B through $C(t)$ and $R_0(t)$. The integrations in (1) and (2) are only over the time in one day for which $E_c(t)/N_0 \geq 0$ dB. Thus, since $E_c(t)/N_0$ is a function of R_c , the theoretical throughputs are functions of R_c also through the integration time intervals.

For completeness, we give soft-decision expressions for $C(t)$ and $R_0(t)$ assuming MPSK signaling on an additive white Gaussian noise (AWGN) channel with two-sided power density $N_0/2$. Let $\{a_i(t)\}_{i=0}^{M-1}$ be M complex functions of time which represent the set of M -ary PSK signals, each of which has energy $E_s(t) = E_c(t) \log_2 M$ at time t . Then [5],

$$C(t) = R_c - \frac{R_c}{M} \sum_{i=0}^{M-1} E\{\log_M[f_i(w, t)]\} \quad (\text{bits/s}) \quad (3)$$

¹Note that implicit in the time-varying capacity or cutoff rate are the existence of codes whose rates are time varying and just less than $C(t)/R_c$ or $R_0(t)/R_c$ (information bits/code bit).

where

$$f_i(w, t) = \sum_{j=0}^{M-1} \exp\left(-\frac{|a_i(t) + w - a_j(t)|^2 - |w|^2}{N_0}\right)$$

and where $E\{\cdot\}$ represents expectation with respect to the zero-mean, normally distributed random variable w which is real with variance $N_0/2$ when $M = 2$, and complex with variance N_0 otherwise. The cutoff rate for the same situation is given [5] by

$$R_0(t) = R_c - R_c \log_M[\gamma(t)] \quad (\text{bits/s}) \quad (4)$$

where

$$\gamma(t) = \sum_{k=0}^{M-1} \exp\left(-\frac{E_s(t)}{N_0} \sin^2\left(\frac{\pi k}{M}\right)\right).$$

We remark that C and R_0 for BPSK and QPSK are equal.

If one wishes to remove the constraint on the modulation type, but maintain only an energy constraint on the signaling scheme, then the appropriate capacity for any two-dimensional (2-D) signal set is given [5] by

$$C(t) = R_s \log_2\left(1 + \frac{C(t)}{R_s N_0}\right) = R_s \log_2\left(1 + \frac{E_s(t)}{N_0}\right). \quad (5)$$

While our emphasis will be on the M -ary PSK signal set as mentioned above, we shall present some results based on the capacity measure given in (5). In the sequel, we shall write C_{EC} (EC for energy constraint) for this latter capacity measure and C_{PSK} for the capacity of a PSK signal set.

We may now define

$$(M^*, R_c^*, B^*) = \arg \max\{\mathcal{T}_X(M, R_c, B)\} \quad (6)$$

where the maximization is over all candidates M, R_c , and B , and where X is C_{PSK} , C_{CE} , or R_0 , depending on the capacity measure adopted. Finding general expressions for the critical points M^* , R_c^* , and B^* in (6) is a rather intractable problem. Instead, we have resorted to numeric computation, the results of which are presented below.

III. ORBITAL SIMULATION MODEL

We now describe assumptions made in calculating C/N_0 profiles in the LEO-to-GEO satellite system. The LEO satellite's orbital period and inclination angle greatly influence the number and duration of contacts to the GEO satellite. Using Kepler's equations of motion [6], the orbital position vector of the LEO satellite is calculated for 200 points per orbit.² The GEO relay satellite's position vector is stationary, so it need only be derived once. Using these two vectors, the pointing vector from the LEO satellite to the GEO satellite is calculated for every LEO position. The angle of the pointing vector is used to determine if the LEO satellite is within view of the GEO satellite. If so, the C/N_0 for the current LEO satellite position is computed.

²Results using greater resolution did not provide any significant increase in C/N_0 resolution since intermediate values were easily interpolated when necessary.

TABLE I
 C/N_0 PROFILE SUMMARIES

B	# of Contacts	$(C/N_0)_{max}$ (dB-Hz)	Duration (minutes)
70	6	62.1, 58, 58.8, 62.2, 60.8, 61.3	28.3, 22.7, 24.2, 27.8, 26.2, 27.3
52	4	65, 65.1, 62.5, 63.6	19, 19.6, 15.9, 17
42	4	66.6, 66.9, 62.4, 64.4	14.9, 15.4, 10.8, 12.9
36	3	67.7, 68.1, 64.5	12.9, 13.4, 9.7
28	2	69.7, 70.3	9.8, 10.3
20	2	71.5, 73	5.6, 7.2
14	1	75.3	4

The calculation of the antenna gains can be modeled in two-dimensional space due to the assumed circular polarization of the antennas involved. The use of circular polarization also increases the power available since polarization losses will be avoided.

The algorithm used is summarized as below. Note that orbital perturbations are not included in the calculations.

- 1) Define the mean motion for each satellite.
- 2) Find the mean anomaly for each satellite.
- 3) Compute the eccentric anomaly for each satellite.
- 4) Compute the true anomaly for each satellite.
- 5) Compute the radial distance to each satellite.
- 6) Solve for the LEO satellite position vector.
- 7) Check for possible contact between the satellites [if none, skip 8) and 9)].
- 8) Calculate LEO antenna gain for current position.
- 9) Compute C/N_0 for the current orbital position.
- 10) Move to next orbital position, go to step 1.

IV. APPLICATION

We assume a LEO satellite with an orbital period of 102.86 min (14 orbits/day) and an inclination angle of 100° . Further, the LEO satellite is assumed to have the following parameters.

- Spin stabilization in a nadir orientation, i.e., the long axis of the satellite intersects the center of the earth.
- Transmitter power³: 3 W.
- Antenna: circularly polarized, helical, nongimbaled, and pointing away from the earth's center. The helical antenna design method used may be found in [7]. We also consider the following 3 dB beamwidths: 70, 52, 42, 36, 28, 20, and 14° . Frequency: S-band (2.2–2.3 GHz).

The GEO satellite assumed is NASA's Tracking and Data Relay Satellite (TDRS) located at 41° west in geostationary orbit. The TDRS parameters assumed are

- G/T : 8.9 dB/K
- antenna: 16 ft parabolic, circularly polarized, and capable of open-loop tracking.

³We remark that T_X scales with transmitter power if the signaling rate is scaled by the same factor. For example, $T_X(3 \text{ W}) = 3T_X(1 \text{ W})$. This is shown in the Appendix.

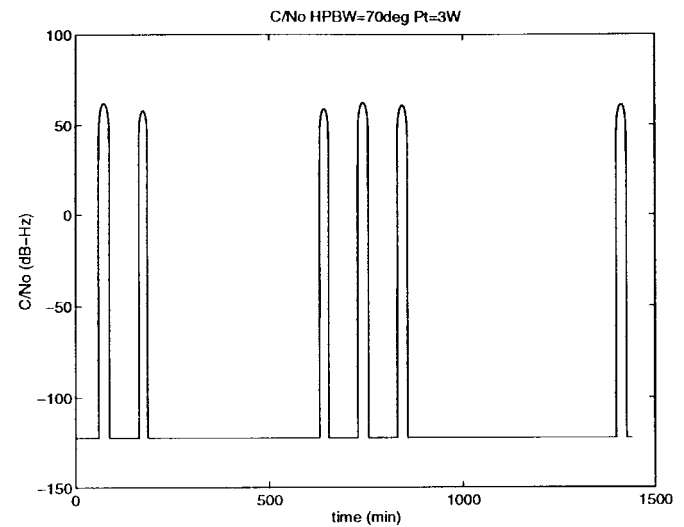


Fig. 1. C/N_0 profile for the 70° case.

The 24 h C/N_0 profile for the 70° LEO satellite antenna case appears in Fig. 1, where it is seen that six contacts are made. Space limitations do not permit us to include the C/N_0 profiles for the other beamwidths, so we summarize in Table I the results for these cases. We observe that while the narrower beamwidths will typically produce fewer contacts with shorter durations on average, greater power per contact is obtained. Thus, it is not clear at this point which is the optimal beamwidth. Hence, the utility of (1) and (2) as we now show.

For $M = 2$, Fig. 2 plots $\mathcal{I}_{C_{PSK}}(M, R_c, B)$ for the values of B given above and for R_c in the range 0–10 M code bits/s (Mcbits/s). The “dips” in the curves correspond to individual E_c/N_0 profiles dropping below the 0 dB threshold as R_c is increased, therefore no longer contributing to the total throughput. We observe that $\mathcal{I}_{C_{PSK}}$ is maximized at about 1.8 Gbits/day for $B = 20^\circ$ and $R_c = 5.2$ Mcbits/s. We remark that the throughput curves for QPSK are identical, as should be expected. As for 8-PSK, $\mathcal{I}_{C_{PSK}}$ is maximized at 1.5 Gbits/day for $B = 20^\circ$ and $R_c = 5.2$ Mcbits/s, although we do not present the throughput curves in this case (they are very similar). Thus, with C_{PSK} as the capacity measure, $M^* = 2$

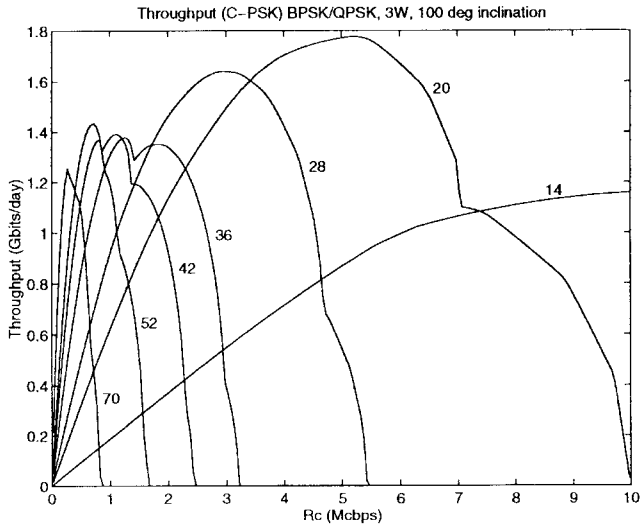


Fig. 2. T_C versus R_c parameterized by antenna 3 dB beamwidths for BPSK and QPSK.

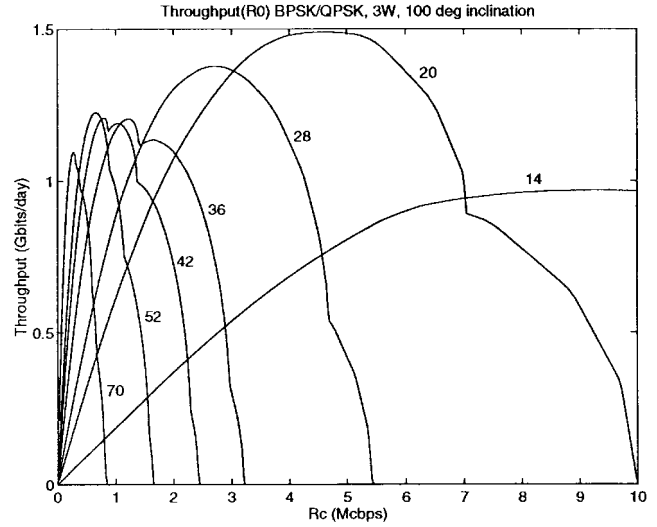


Fig. 4. T_{R_0} versus R_c parameterized by antenna 3 dB beamwidths for BPSK and QPSK.

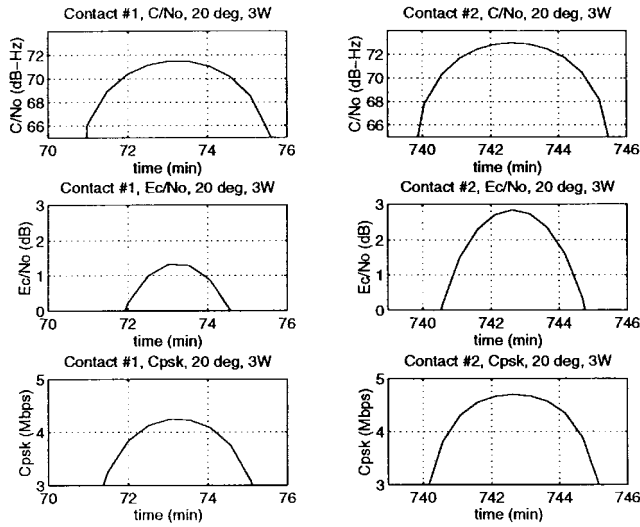


Fig. 3. E_c/N_0 and C profiles for the optimum scenario.

or 4, $B^* = 20^\circ$, and $R_c^* = 5.2$ Mcbits/s. (Hence, for BPSK, $R_s^* = 5.2$ Msym/s, and for QPSK, $R_s^* = 2.6$ Msym/s.)

The E_c/N_0 profiles corresponding to the optimal R_c and B are plotted in Fig. 3, together with their corresponding C_{PSK} and C/N_0 profiles. In this figure and in the computation of C_{PSK} and T_{R_0} , 3 dB was subtracted from the E_c/N_0 profiles to simulate implementation loss (e.g., timing jitter, pointing errors, orbital perturbations). The achievable throughput is the area under the $C_{PSK}(t)$ curves for the time corresponding to $E_c(t)/N_0 \geq 0$ dB. Observe that the optimal R_c corresponds to the low SNR region of operation.

Fig. 4 plots T_{R_0} versus R_c for $M = 2$ for the set of beamwidths B given above. We observe that T_{R_0} is maximized at about 1.5 Gbits/day for $B = 20^\circ$ and $R_c = 4.5$ Mcbits/s. Again, the QPSK curves are identical. For 8-PSK (curves not shown), T_{R_0} is maximized at 1.25 Gbits/day for $B = 20^\circ$ and $R_c = 5.25$ Mcbits/s. Thus, using the R_0 criterion, $M^* = 2$ or 4, $B^* = 20^\circ$ and $R_c^* = 4.5$ Mcbits/s which is

in close agreement with the C_{PSK} criterion. Note also that the maximum is essentially achieved when $R_c = 5.2$ Mcbits/s since the $B = 20^\circ$ curve possesses a broad maximum.

For the constrained-energy capacity criterion C_{EC} , we must make a minor adjustment in our presentation since code bits are not defined in this case (only code symbols make sense here since no particular modulation format is assumed). Thus, we must plot $T_{C_{EC}}$ versus R_s instead of R_c . For the same reason, the requirement $E_c(t)/N_0 \geq 0$ dB is not meaningful, although a constraint on $E_s(t)/N_0$ would be. Because $C_{EC} \approx C_{QPSK}$ in the E_s/N_0 region of interest (low to medium E_s/N_0 for this power-limited scenario), we shall require $E_s(t)/N_0 \geq 3$ dB to match the QPSK case. Fig. 5 presents the resulting throughput curves. We observe that $T_{C_{EC}}$ is maximized at about 2.1 Gbits/day for $B = 20^\circ$ and $R_s = 2.2$ Msym/s as compared to 1.8 Gbits/day and $R_s = 2.6$ Msym/s for $T_{C_{PSK}}$ with $M = 4$. Thus, an additional 17% in throughput (0.3 Gbits/day) would be available for a signaling set more exotic (e.g., variable size) than QPSK or BPSK.

We repeated the above scenario for a 60° LEO satellite inclination angle and for the C_{PSK} and R_0 criteria. We found again that $M^* = 2$ and 4, and $B^* = 20^\circ$. For C_{PSK} , we found $R_c^* = 5.5$ Mcbits/s and $T_{C_{PSK}}^* = 2.0$ Gbits/day, and for R_0 , these numbers were $R_c^* = 4.5$ Mcbits/s and $T_{R_0}^* = 1.7$ Gbits/day. Thus, increased throughput is available at this inclination. Of course, as the orbital inclination decreases further, we can expect the achievable throughput to increase until it achieves a maximum at zero inclination (equatorial orbit).

We finally remark in this section that, for BPSK and QPSK, the optimal code bit rate R_c^* can be estimated for any beamwidth B without having to plot the T_X versus R_c curves of Figs. 2 and 4. (There is a similar formula for 8-PSK, but it is unimportant to us since the maximum throughput is achieved only by BPSK and QPSK.) Let N_B be the number of contacts for a LEO satellite using an antenna with beamwidth B , and let $A_0(k), k = 1, 2, \dots, N_B$, be the maximum C/N_0 value for the k th contact after the 3 dB implementation loss has been

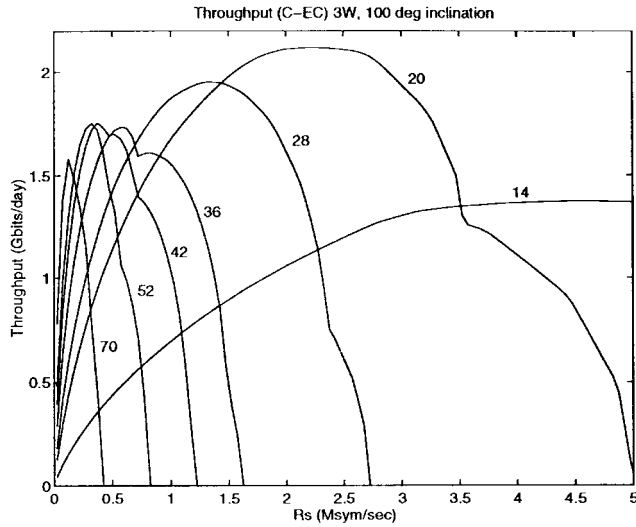


Fig. 5. $\mathcal{T}_{C_{EC}}$ versus R_s parameterized by antenna 3 dB beamwidths.

TABLE II
COMPARISON OF OPTIMAL R_c^*

B	R_c^* (Mcbps) (Figs. 2, 4)		R_c^* (Mcbps) (Eq. 7)	
	C_{PSK}	R_0	C_{PSK}	R_0
70	0.28	0.28	0.32	0.29
52	0.73	0.65	0.71	0.63
42	1.13	0.80	0.94	0.84
36	1.28	1.23	1.38	1.22
28	2.93	2.73	2.71	2.41
20	5.23	4.46	4.61	4.10
14	11.6	9.03	9.17	8.15

subtracted. Then we find that R_c^* can be approximated as

$$R_c^* \simeq \frac{1}{N_B} \sum_{k=1}^{N_B} \lambda A_0(k) \simeq \frac{1}{N_B} \sum_{k=1}^{N_B} A_0(k)/2 \quad (7)$$

where $\lambda = 0.54$ for C_{PSK} and $\lambda = 0.48$ for R_0 . To verify this formula, we list in Table II for all beamwidths considered here the actual R_c^* obtained from Figs. 2 and 4, together with R_c^* predicted by the formula above. We observe that in all cases there is close agreement between the two. For example, assuming the C criterion and the $B = 28$ case, (7) yields $R_c^* \simeq 2.71$ as compared to $R_c^* = 2.93$ from Fig. 2. The next section gives the origin of this formula.

V. THROUGHPUT OF SELECTED CODES

A. Preliminaries

The main result of the previous section is essentially that, for the given scenario, at an orbital inclination of 100° (60°), a code exists for which 1.8 Gbits/day (respectively,

2.0 Gbits/day) may be reliably transmitted when $B = 20^\circ$, $M = 2$ or 4 , $R_c \simeq 5.2$ Mcbits/s. In this section, we estimate the throughput achievable by practical fixed- and variable-rate coding schemes. The throughput here is the number of information bits transmitted while $E_c(t)/N_0 \geq 0$ dB and with a probability of error less than some prescribed value.

If we were to apply a code to the C -optimal ($B = 20^\circ$, $R_c = 5.2$ Mcbits/s) E_c/N_0 profile of the previous section to calculate its throughput, the computation time would be unmanageable because the number of code bits for the two contacts for this case is approximately (2.3 min + 4.1 min) (60 s/min) (5.2 Mcbits/s) $\simeq 2 \times 10^{10}$ code bits (see Fig. 3). Thus, we shall instead consider a single contact in the total C/N_0 profile, and approximate that contact by a function of time which lends itself to analysis and provides insight into the results presented above. Specifically, we shall assume a C/N_0 profile (actually, contact) of the form

$$C(t)/N_0 = A_0 \exp(-t^2/2\sigma^2) \quad (8)$$

where the maximum value A_0 of $C(t)/N_0$ occurs at time $t = 0$ by our choice of time origin, and σ is a measure of the duration of the communication link. Note that the shape of (8) approximates well the shape of the individual contacts of Fig. 3.

The C/N_0 profile of (8) gives rise to an E_c/N_0 profile through the chosen code bit rate R_c :

$$E_c(t)/N_0 = (A_0/R_c) \exp(-t^2/2\sigma^2). \quad (9)$$

As mentioned, we shall assume communication is possible only when $E_c(t)/N_0 \geq 0$ dB. The interval $[-t_0, t_0]$ for which this is true is easily found by solving for t_0 in the equation $E_c(t_0)/N_0 = 1$, yielding

$$t_0 = \sigma \sqrt{2 \ln(A_0/R_c)} \quad (10)$$

which exists only if $R_c \leq A_0$.

The theoretical throughputs of interest here are ($C = C_{PSK}$ hereafter)

$$\mathcal{T}_C = \int_{-t_0}^{t_0} C(t) dt \quad (\text{bits}) \quad (11)$$

$$\mathcal{T}_{R_0} = \int_{-t_0}^{t_0} R_0(t) dt \quad (\text{bits}), \quad (12)$$

We find it instructive to find M^* and R_c^* corresponding to (8)–(12). In obtaining the critical points M^* and R_c^* in (11) and (12), we have found it convenient to decouple the throughput expressions for \mathcal{T}_C and \mathcal{T}_{R_0} from A_0 and σ in the following manner. Define $t' = t/\sigma$, $t'_0 = t_0/\sigma$, $R'_c = R_c/A_0$, $C'(t) = C(t)/A_0$, and $R'_0(t) = R_0(t)/A_0$. Then, it is easy to show

$$\mathcal{T}_C = \sigma A_0 \mathcal{T}'_C \quad (\text{bits}) \quad (13)$$

$$\mathcal{T}_{R_0} = \sigma A_0 \mathcal{T}'_{R_0} \quad (\text{bits}) \quad (14)$$

where

$$\mathcal{T}'_C = \int_{-t'_0}^{t'_0} C'(t') dt' \quad (\text{bits}) \quad (15)$$

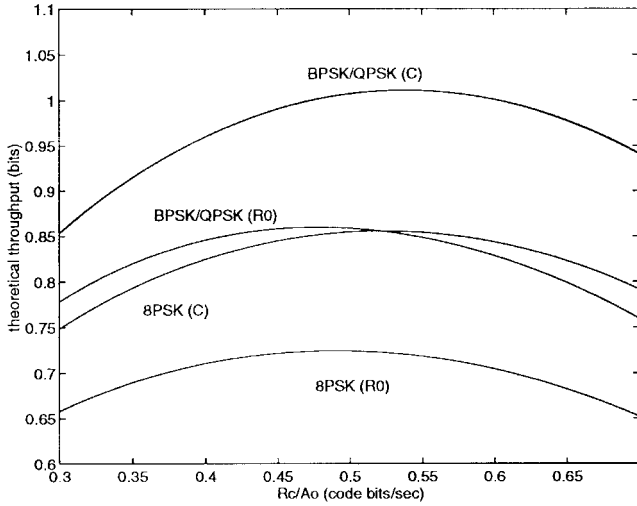


Fig. 6. \mathcal{T}'_C versus R'_c and \mathcal{T}'_{R_0} versus R'_c for BPSK, QPSK, and 8-PSK.

$$\mathcal{T}'_{R_0} = \int_{-t'_0}^{t'_0} R'_0(t') dt' \quad (\text{bits}) \quad (16)$$

are functions of M and R'_c , but are independent of A_0 and σ . Now, note from (13) and (14) that maximizing \mathcal{T}'_C and \mathcal{T}'_{R_0} over M and R'_c is equivalent to maximizing \mathcal{T}_C and \mathcal{T}_{R_0} over M and R_c . This fact is useful since the former quantities are independent of A_0 and σ . The latter throughput quantities may be obtained from the former via the factor σA_0 per (13) and (14).

Fig. 6 plots \mathcal{T}'_C versus R'_c for $M = 2, 4, 8$ from which it is observed that $M^* = 2$ or 4 , $R'_c{}^* = 0.54$ (or $R_c^* = 0.54A_0$), and $\mathcal{T}'_C{}^* = 1.01$ (or $\mathcal{T}_C^* = 1.01\sigma A_0$). When R_0 is instead used as our optimality criterion, we have from Fig. 6 that $M^* = 2$ or 4 , $R'_c{}^* = 0.48$, and $\mathcal{T}'_{R_0}{}^* = 0.86$.

The E_c/N_0 profile which results from dividing (8) by $R_c^* = \lambda A_0$ ($\lambda = 0.54$ for \mathcal{C}_{PSK} and $\lambda = 0.48$ for R_0) is given by

$$(E_c(t)/N_0)^* = \frac{1}{\lambda} \exp(-t^2/2\sigma^2). \quad (17)$$

We observe that in each case $(E_c/N_0)_{\text{max}} = (E_c(0)/N_0)^* \simeq 2$, and hence we shall assume hereafter that the optimum E_c/N_0 profile is $(E_c(t)/N_0)^* = 2 \exp(-t^2/2\sigma^2)$; equivalently, we let $R_c^* = A_0/2$. It is from this result that (7) was derived.

For later comparison with the code scheme throughputs, we now compute the theoretical throughputs \mathcal{T}_C and \mathcal{T}_{R_0} at their respective R_c^* and M^* . Suppose t_0 corresponds to N 8 bit code symbols. Then $t_0 = 8N/R_c$ s since the code symbol rate is $R_c/8$ symbols/s. It then follows from (10) and $R_c^* = A_0/2$ that $\sigma A_0 = 16N/\sqrt{2 \ln 2}$ and, since $\mathcal{T}'_C{}^* = 1.01$ and $\mathcal{T}'_{R_0}{}^* = 0.86$, we have from (13) and (14) that

$$\mathcal{T}_C = 1.01 \left(\frac{16N}{\sqrt{2 \ln 2}} \right) \quad (\text{bits}) \quad (18)$$

$$\mathcal{T}_{R_0} = 0.86 \left(\frac{16N}{\sqrt{2 \ln 2}} \right) \quad (\text{bits}). \quad (19)$$

Thus, for example, when $N = 15\,000$ symbols, $\mathcal{T}_C = 205\,875$ bits and $\mathcal{T}_{R_0} = 175\,300$ bits.

B. Throughput Calculations

Following the results above, we now examine the throughput achievable by several coding schemes. Thus, we assume an E_c/N_0 profile of $E_c(t)/N_0 = 2 \exp(-t^2/2\sigma^2)$ and BPSK or QPSK signaling. Further, we assume that this profile is known *a priori* to the variable-rate scheme since it is computable to reasonable accuracy from the known orbits of the communicating satellites. The following schemes are considered.⁴

- 1) Rate-1/2, constraint length-7 convolutional (inner) code concatenated with a (255, 223) Reed-Solomon (RS) (outer) code over GF(256) [8].
- 2) Variable-rate (1/2, 2/3, 3/4, 4/5),⁵ constraint length-7 convolutional (inner) code concatenated with a variable rate (255, k) RS (outer) code ($k = 223, 225, \dots, 255$).
- 3) Variable-rate (1/2, 2/3, 3/4, 4/5), constraint length 7-convolutional (inner) code concatenated with a fixed rate (255, 223) RS (outer) code.

We shall require a decoded outer RS codeword probability of $P_{cw} \leq 10^{-5}$. For code 2, k was initially set to 223, and the rate of the inner code and then the outer code was varied until $P_{cw} \leq 10^{-5}$ was attained. For both the fixed and variable-rate code schemes, the throughputs \mathcal{T}_a , $a \in \{1, 2, 3\}$, are the number of information bits corresponding to the RS codewords received in the interval $[-t_0, t_0]$ which achieve $P_{cw} \leq 10^{-5}$.

Assuming that byte interleaving has been employed to make the channel appear memoryless to the RS decoder, the codeword error rate P_{cw} is given [8] by

$$P_{cw} = \sum_{j=e+1}^{255} \binom{255}{j} P^j (1-P)^{255-j} \quad (20)$$

where $e = \lfloor (255 - k/2) \rfloor$ is the error-correction bound for the outer RS code. The quantity P is the 8 bit symbol error probability at the output of the convolutional (Viterbi) decoder. No simple analytical technique is available for this quantity, but simulations have shown that P is in the range of $2p-4p$ for the above set of rates, where p is the bit-error rate of the Viterbi decoder. We shall use the bound $P = 4p$ in our calculations. The bit-error rate p is known [8] to be upper bounded and closely approximated as

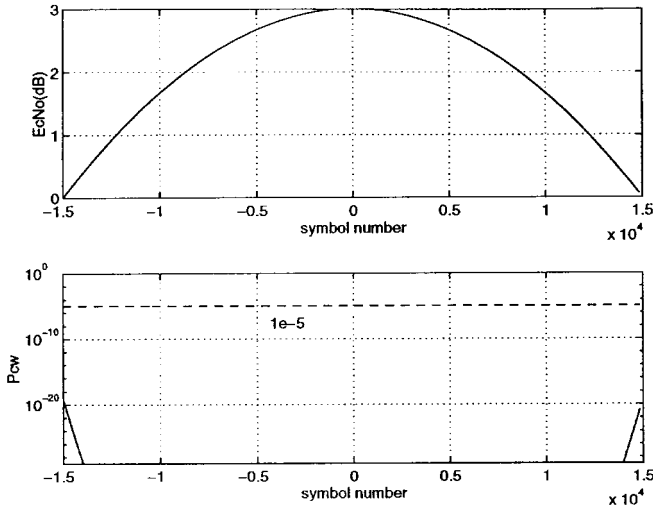
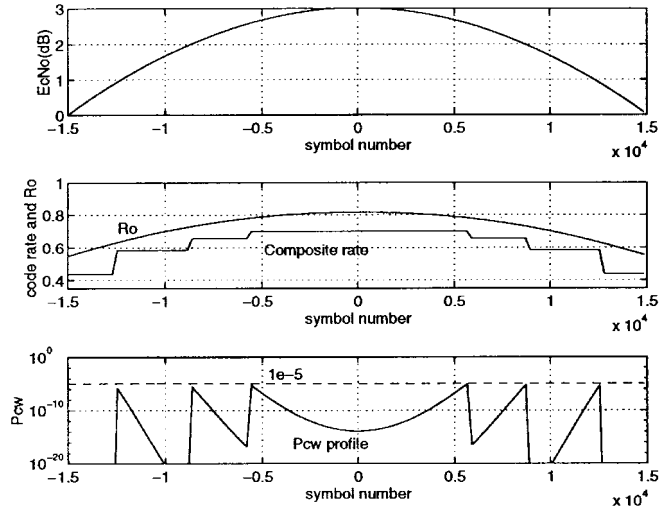
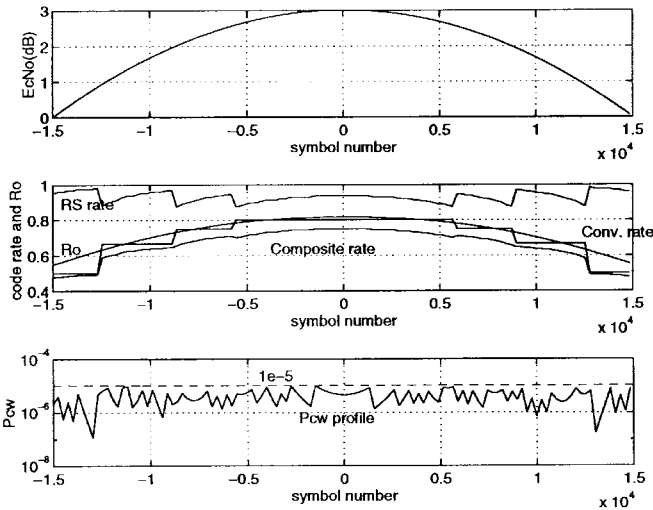
$$p \simeq \frac{1}{k'} \sum_{d=d_f}^{\infty} b_d Q \left(\sqrt{\frac{2dE_c}{N_0}} \right) \quad (21)$$

where the convolutional code has rate k'/n' , minimum free distance d_f , and information weight spectrum $\{b_d\}$. Although E_c is time varying, we assume that it is relatively constant over the duration of a codeword, as will be the case in practice where several thousand codewords are transmitted per second.

Fig. 7 plots the P_{cw} profiles for fixed-rate scheme 1 with $N = 15\,000$ symbols ($t_0 = 8(15\,000)/R_c$ ss). We

⁴Note that the first code is the CCSDS standard concatenated code adopted by NASA and ESA [8], and the other two codes are variable-rate versions of this code. (CCSDS: Consultative Committee for Space Data Systems.)

⁵For convolutional code rates larger than 1/2, we assume punctured coding [10]. Also, we considered higher rate codes, e.g., 5/6, 6/7, \dots , but the P_{cw} requirement was never achievable at these rates.

Fig. 7. P_{cw} profile for code 1.Fig. 9. P_{cw} profile for code 3 together with its code rate profile.Fig. 8. P_{cw} profile for code 2 together with its code rate profile.

note that in the figure, $P_{cw} \leq 10^{-5}$ in the interval $[-15000, 15000]$ so that, allowing that last 255-byte codeword to extend beyond the 30000th symbol, we have $T_1 = \lceil (30000/255) \rceil (1/2)(223)(8) = 105256$ bits. Using the capacity criterion, we observe an efficiency of $\mathcal{E}_{C,1} = T_1/T_C = 0.51$. For the cutoff rate criterion, we observe an efficiency of $\mathcal{E}_{R_0,1} = T_1/T_{R_0} = 0.60$.

Fig. 8 plots the P_{cw} profile for scheme 2 whose jagged nature is a result of the changing of code rates in discrete steps, as is also illustrated in the figure. The throughput for scheme 2 can be computed as

$$T = 8(255) \sum_{n=1}^{N_{cw}} r(n) \quad (22)$$

where N_{cw} is the number of codewords transmitted in the interval $[-15000, 15000]$ and $r(n)$ is the composite (convolutional plus RS) rate of the n th codeword. From this, we obtain $T_2 = 158180$ bits. The efficiencies for this code are then $\mathcal{E}_{C,2} = T_2/T_C = 0.77$ and $\mathcal{E}_{R_0,2} = T_2/T_{R_0} = 0.90$.

Finally, Fig. 9 presents the P_{cw} profile for scheme 3. The throughput for scheme 3 computed from (22) yields $T_3 = 148960$ bits. The efficiencies for this code are then $\mathcal{E}_{C,3} = T_3/T_C = 0.72$ and $\mathcal{E}_{R_0,3} = T_3/T_{R_0} = 0.85$. Thus, we observe that little is lost in throughput by fixing the rate of the RS code to 223/255. This is not surprising since the RS code rates in code schemes 2 and 3 are all very high.

C. Discussion

Based on the above \mathcal{C} and R_0 analysis, our assumption to this point has been that $R_c = A_0/2$ is optimal (equivalently, $(E_c/N_0)_{\max} = 3$ dB is optimal). To check whether this is true for practical codes, we repeated the above computations for $R_c = A_0/3.162$ ($(E_c/N_0)_{\max} = 5$ dB) and $R_c = A_0/1.259$ ($(E_c/N_0)_{\max} = 1$ dB). Note that in the first situation, R_c is decreased relative to $R_c = A_0/2$, so that we would expect t_0 to increase. This is easily verified from (10): $t_{0,5\text{dB}} = \sigma\sqrt{2\ln(3.162)}$ as compared to $t_{0,3\text{dB}} = \sigma\sqrt{2\ln(2)}$. However, the number of symbols $N_{5\text{dB}}$ corresponding to $t_{0,5\text{dB}}$ need not increase, as can be seen from

$$\begin{aligned} N_{5\text{dB}} &= t_{0,5\text{dB}} R_{c,5\text{dB}} / 8 \\ &= \left(\frac{\sqrt{2\ln(3.162)}}{\sqrt{2\ln(2)}} t_{0,3\text{dB}} \right) \left(\frac{2}{3.162} R_{c,3\text{dB}} \right) / 8 \\ &= (0.815)(t_{0,3\text{dB}} R_{c,3\text{dB}} / 8) \\ &= (0.815)(15000) \\ &= 12225 \end{aligned}$$

which is less than $N_{3\text{dB}} = 15000$. We may similarly show $N_{1\text{dB}} = 13736$.

Given that $N_{5\text{dB}}$ and $N_{1\text{dB}}$ are both less than $N_{3\text{dB}}$, it is evident that the fixed-rate codes will yield a decreased throughput for $(E_c/N_0)_{\max} = 1$ and 5 dB. Further, we cannot expect an increased throughput for any of the three codes when $(E_c/N_0)_{\max} = 1$ dB since $N_{1\text{dB}} < N_{3\text{dB}}$ and E_c/N_0 in this case is always smaller than that of the 3 dB case. These two points are verified in Table III which lists the throughputs and R_0 efficiencies of all three codes for the $(E_c/N_0)_{\max} = 1$,

TABLE III
THROUGHPUTS AND R_0 -EFFICIENCIES

Code	Throughput/Efficiency		
	$(E_c/N_0)_{max} = 1$ dB	$(E_c/N_0)_{max} = 3$ dB	$(E_c/N_0)_{max} = 5$ dB
1	96,336/0.72	105,256/0.60	85,632/0.53
2	115,000/0.86	158,180/0.90	146,890/0.91
3	107,340/0.80	148,960/0.85	136,030/0.84

3, and 5 dB situations.⁶ When $(E_c/N_0)_{max} = 5$ dB, code schemes 2 and 3 offer the possibility of improved throughput since the $P_{cw} \leq 10^{-5}$ criterion may now be met with higher codes rates. However, as seen in Table III, the throughput for each code is maximum when $(E_c/N_0)_{max} = 3$ dB, as indicated by the theory (equivalently, the optimal code bit rate for practical codes $R_{c,pc}^*$ is equal to $A_0/2$). When more than a single contact is involved, as was the case in Section IV, we conjecture that $R_{c,pc}^* = A_0/2$ generalizes to an average of the values $A_0(k)/2$, analogous to (7).

We would like now to couple the results of the present section with those of Section IV to estimate the LEO-to-GEO throughput achievable by codes 1–3. Ostensibly, we cannot simply apply the efficiencies $\mathcal{E}_{R_0,a} = \mathcal{T}_a/\mathcal{T}_{R_0}$ computed above to the throughput values of Section IV because these efficiencies apply only to the single-contact case for which $(E_c/N_0)_{max} = 3$ dB (equivalently, $R_c = A_0/2$). However, as seen in Table III, the code efficiencies do not vary widely with $(E_c/N_0)_{max}$. Hence, when multiple contacts are present in an E_c/N_0 profile with differing $(E_c/N_0)_{max}$'s, the throughput \mathcal{T}_a for code scheme a may be estimated by multiplying the theoretical throughput \mathcal{T}_{R_0} by the average of the Table III efficiencies.

For example, from Table I, for the two contacts obtained with the 20° antenna, the two values of $(E_c/N_0)_{max}$ are calculated as $71.5 - 3 - 10 \log_{10}(4.5 \text{ Mbits/s}) = 1.96$ dB and $73 - 3 - 10 \log_{10}(4.5 \text{ Mbits/s}) = 3.46$ dB. From Table III, the average efficiency for code 2 is about 0.88 in this range. Thus, we can expect this code to achieve about 88% of the throughput predicted by the R_0 analysis of Section IV, that is, a throughput of about 1.3 Gbits/day. Similarly, we can expect the fixed rate codes to achieve about 60% of $\mathcal{T}_{R_0} = 1.5$ Gbits/day, or 0.9 Gbits/day.

VI. CONCLUSION

We have given a technique based on capacity and cutoff rate for designing a LEO-to-GEO satellite link with the goal of maximizing the daily throughput. The approach leads to an optimal LEO satellite antenna beamwidth, an optimal channel signaling rate, and an optimal signal set size for MPSK. The analysis of selected coding schemes indicates that about 90% of the throughput predicted by the R_0 analysis, or 77% of that predicted by the \mathcal{C} analysis, is achievable in practice.

⁶We list the R_0 efficiencies as opposed to the \mathcal{C} efficiencies since, as demonstrated above, the R_0 criterion gives a closer approximation to the actual efficiencies for the codes considered.

This design approach is generalizable in that it may be applied to any situation for which the communication link is of short duration and is time varying in a (mostly) deterministic way. For example, the above analysis may be repeated for the scenario where data are transmitted directly to the ground from the LEO satellite. Alternatively, it may be applied to a situation in which two or more LEO satellites in relative motion are communicating. Lastly, this design technique may be applied to meteor burst channels which fit the above description. Some work in this latter area is reported in [10].

APPENDIX

We show here that, as mentioned in a footnote in Section IV, the theoretical throughputs \mathcal{T}_{R_0} and $\mathcal{T}_{\mathcal{C}}$ scale with transmitter power when the signaling rate is scaled by the same factor. Our discussion will focus on \mathcal{T}_{R_0} ; the proof for $\mathcal{T}_{\mathcal{C}}$ is essentially identical.

Clearly, C/N_0 scales with transmitter power. Now, let α represent that scale factor, and define $\tilde{C}/N_0 = \alpha C/N_0$. We shall show that, when operating at a new signaling rate $\tilde{R}_s = \alpha R_s$, the throughput is also changed by the factor α . Observe that by also scaling the signaling rate, E_s remains constant: $\tilde{E}_s = \tilde{C}/\tilde{R}_s = \alpha C/\alpha R_s = E_s$. Hence, $\gamma(t)$ will remain constant [see (4)]: $\tilde{\gamma}(t) = f(\tilde{E}_s) = f(E_s) = \gamma(t)$. Now, observe that the throughput resulting from the scaling of C and R_s by α simplifies as

$$\begin{aligned} \tilde{\mathcal{T}}_{R_0} &= \int_{\text{one day}} \tilde{R}_0(t) dt \\ &= \tilde{R}_c \int_{\text{one day}} 1 - \log_M[\tilde{\gamma}(t)] dt \\ &= \alpha R_c \int_{\text{one day}} 1 - \log_M[\gamma(t)]; dt \\ &= \alpha \mathcal{T}_{R_0}. \end{aligned}$$

ACKNOWLEDGMENT

The authors would like to acknowledge the helpful discussions of Dean W. Osborne of the University of Texas at Dallas and Prof. S. Horan of New Mexico State University, Las Cruces, who proposed the nongimbaled antenna scenario. Prof. Horan wrote the original orbital simulation program which was modified for this work. They would also like to acknowledge the programming help of J. Moser. Finally, the comments of the reviewers which helped to improve this paper are appreciated.

REFERENCES

- [1] G. Kronmiller and J. Chitwood, "Concept for efficient TDRSS support to the small satellite user community," NASA Goddard Space Flight Cen., Code 531 and Code 737, Jan. 1993.
- [2] S. Horan and T. Minnix, "Small satellite access of the space network," in *Proc. Int. Telemetry Conf.*, San Diego, CA, 1994.
- [3] J. Wozencraft and I. Jacobs, *Principles of Communication Engineering*. New York: Wiley, 1965, ch. 5.
- [4] B. Kopp, "An analysis of carrier jitter in an MPSK receiver utilizing map estimation," Ph.D. dissertation, New Mexico State Univ., Las Cruces, 1994.
- [5] S. Wilson, *Digital Modulation and Coding*. Englewood Cliffs, NJ: Prentice-Hall, 1996.

- [6] J. Miyamoto, "Position and velocity as a function of time," in *Orbital Mechanics*, V. Chobotov, Ed. Washington, DC: AIAA, 1991, pp. 47-97.
- [7] W. Stutzman and G. Thiele, *Antenna Theory and Design*. New York: Wiley, 1981, ch. 6.
- [8] S. Wicker, *Error Control Systems for Digital Communication and Storage*. Englewood Cliffs, NJ: Prentice-Hall, 1995.
- [9] D. Haccoun and G. Begin, "High-rate punctured convolutional codes for Viterbi and sequential decoding," *IEEE Trans. Commun.*, pp. 1113-1125, Nov. 1989.
- [10] W. Ryan, "Optimal signaling for meteor burst channels," *IEEE Trans. Commun.*, pp. 489-496, May 1997.



Paul A. Quintana received the B.S. and M.S. degrees from New Mexico State University, Las Cruces, in 1992 and 1994, respectively.

From 1995 to 1996, he worked as an ASIC product development engineer at Texas Instruments. His work at Texas Instruments involved the development of new test procedures for high speed ASIC designs, as well as the characterization of new CMOS technologies. In September 1996, he joined Lockheed-Martin Wideband Systems, San Jose, CA, as a Senior Systems Engineer. He is currently involved in the research and development of wireless airborne network communications using both ATM and internally developed protocols.



William E. Ryan received the B.S.E.E. degree from Case Western Reserve University, Cleveland, OH, in 1981 and the M.S. and Ph.D. degrees in electrical engineering from the University of Virginia, Charlottesville, in 1984 and 1988, respectively.

He has held positions at The Analytic Sciences Corporation, Ampex Corporation, and Applied Signal Technology prior to his present position at New Mexico State University, Las Cruces, where he is an Associate professor in the Department of Electrical and Computer Engineering. His research interests

are in coding and signal processing for data transmission and storage. These topics include algebraic and trellis codes, concatenated codes with iterative (turbo) decoding, constrained codes, and linear and nonlinear feedforward and decision-feedback equalizers.

Dr. Ryan was the recipient of an NSF Research Initiation Award in 1994.



Li Han received the B.S. degree in Opto-Electronics from Tianjin University, Tianjin, P.R. China, in 1989, and the M.S.E.E. degree from the New Mexico State University, Las Cruces, in 1995.

From 1989 to 1992 he was employed by Power and Dispatching Communication Bureau, Ministry of Energy, Beijing, P.R. China, working on optical fiber communications systems.

In January 1996, he joined Samsung Semiconductor, San Jose, CA, where he worked on a system simulation of a PRML magnetic recording channel.

Since July 1996, he has been with Samsung Information Systems America, Hard Disk Drive Center, San Jose, where he works on the simulation design and performance analysis of error correction codes (ECC) for a hard disk drive controller chip. His current interests include digital communications, ECC, and signal processing.